GEOPHYSICAL TRANSACTIONS 2000
Vol. 43. Number 1. pp. 47 – 63

Quality controlled resistivity inversion in cavity detection

Zsuzsanna NYÁRI*

Cavity detection is a common problem in engineering geophysics. Resistivity methods have been widely used for such tasks since the development of multi-electrode measuring systems. These new computer controlled data collecting systems provide large amounts of data in a short time. This paper presents the latest theoretical developments of ELGI in processing geoelectric data for the use of near surface cavity detection.

When, apart from the location, the size and the depth of cavities are needed an inversion method based on 2-D analytic model calculations can be used; this method also gives their uncertainty. After numeric tests this inversion method has been successfully applied on field data.

To improve the reliability of the cavity parameters a simultaneous inversion method has been developed whose inputs are two datasets measured by different electrode arrays (dipole–dipole and Wenner) along the same profile. The results of the numeric investigations prove that this processing method gives more reliable solutions than the simple inversion method.

Keywords: resitivity, electrodes, two-dimensional models, cavity, inversion, engineering geophysics

1. Introduction

Near surface cavities mean real danger for traffic and buildings. It is a serious task for engineering geophysics to locate such cavities and it is often necessary to determine reliably their dimensions. Resistivity measurements have been more widely used for such problems since the development of multi-electrode measuring systems, which provide fast data collection.

Resistivity measurements are carried out along a profile where data measured at different electrode separations represent different depths of investigation. The result of the measurement is a 2-D pseudo-section with the raw resistivity data. These pseudo-sections can be processed by FD or FE inversion methods such as was done, for example, by DEY and MORRISON [1979]. BARKER [1992] invented a fast inversion reconstruction method based on a quasi-Newton procedure using only one iteration step. LOKE and BARKER [1996] improved this process and inserted it into an inversion algorithm. Us-

* Eötvös Loránd Geophysical Institute of Hungary, H-1145 Budapest, Kolumbusz u. 17–23
Manuscript received (revised version): 22 September, 1999.

ing FD inversion methods the geoelectric characteristics of the investigated area can be correctly mapped and the anomalies caused by cavities can be reliably marked. GYULAI [1996–1997] invented a 1.5-D FD inversion method especially for cavity detection.

An inversion method whose forward calculation is carried out using the analytic solution of the 2-D cavity model has been developed in order to give rapidly and reliably the positions and size of the investigated objects. This process provides the parameters (location, size, depth) of the cavities along the profile. It is also possible to calculate the reliability values of the model parameters.

Joint inversion uses two (or more) independent methods for measuring along the profile. If joint inversion is applied the investigated parameters can be more correctly estimated than in the case of single inversion. DOBRÓKA et al. [1991] developed a joint inversion algorithm for seismic and resistivity data in the case of layered earth investigations. A method in which the components of the inversion are two datasets measured by two different electrode configurations has a similar effect on the estimated parameters as does joint inversion. GYULAI [1998] used that so-called simultaneous inversion based on 1.5-D forward calculation for cavity detection with dipole–dipole and pole–pole data. My paper will present a simultaneous inversion method based on analytic modelling of dipole–dipole and Wenner data.

2. Data processing with inversion

The inversion algorithm applied here was based on the linearized, qualified inversion method developed by DOBRÓKA et al. [1991] using the Marquard algorithm and L_2 norm. This algorithm has been improved for the particular purpose of cavity detection using 2D analytic forward calculation.

As the first step of the inversion one has to define a model and give its initial parameters:

$$\overline{X} = (p_1,\ldots,p_n) \tag{1}$$

$\overline{X}$: vector of model parameters
p_j: model parameter
n: number of model parameters

In the test the 2-D geological model was a horizontal, infinite length cylinder with infinite resistivity laid in uniform halfspace (*Fig. 1*). The parameters of the model are: resistivity of the earth (ρ_1), location of the cavity along

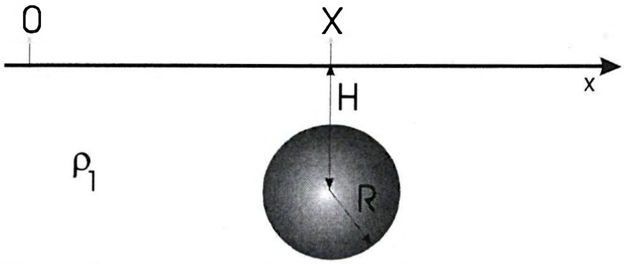

Fig. 1. The 2-D geological model for the inversion
1. ábra. 2-D geológiai modell az inverzió céljára

the profile (x), depth of the midpoint of the cylinder (H), radius of the cylinder (R). In the case of more cavities along the profile the number of parameters will increase by three times the cavity number. Forward calculation is carried out using the parameter vector defined in (1) and the $\bar{s}$ vector of the measured data:

$$Y_i^{cal} = Y(\overline{X}, s_i) \tag{2}$$

$i = 1,2,..,m$
m: number of measured data
s_i: i^{th} measured value
Y: response function

When function Y is the non-linear function of the parameter vector a linearization process is conventional. The first order Taylor expansion of Y is given by:

$$Y_i^{calc} = Y_i^0 + \sum_{j=1}^{n} \left(\frac{\partial Y_i^{calc}}{\partial x_j} \right)_{\overline{X}=\overline{X}_0} \delta x_j \tag{3}$$

$\overline{X}_0$: vector of initial model parameters
$Y_i^{(0)} = Y(X_0, s_i)$

The error vector $\bar{e}$ gives the difference between the response functions of the observed and the calculated data:

$$\bar{e} = \bar{y} - \underline{\underline{G}}\bar{x} \tag{4}$$

where:

$$y_i = \frac{Y_i^{obs} - Y_i^0}{Y_i^{obs}} \qquad x_j = \frac{\delta X_j}{X_j^0} \qquad G_{ij} = \frac{X_j^0}{Y_i^{calc}} \left(\frac{\partial Y_i^{calc}}{\partial X_j} \right)_{\overline{X}=\overline{X}_0}$$

Minimizing the error vector according to L_2 norm leads to a linear equation system:

$$\underline{\underline{G}}^T \underline{\underline{G}} \bar{x} = \underline{\underline{G}}^T \bar{y} \tag{5}$$

The Marquard-Levenberg solution of (5) is:

$$\bar{x} = \left(\underline{\underline{G}}^T \underline{\underline{G}} + \lambda I\right)^{-1} \underline{\underline{G}} \bar{y} \tag{6}$$

I: unit matrix

λ: damping factor

To decrease the errors of linearization several iteration steps are needed.

Forward calculation

The potentials of the uniform halfspace (7) and the 2D cylinder (8) with infinite length and resistivity for infinite length line electrodes were calculated by LÖSCH et al. [1979].

$$\begin{aligned} &V_0(C, P_{11}, \ldots, P_{1q}, P_{21}, \ldots, P_{2q}) = \\ &= \frac{I \cdot \rho_1}{\pi q} \left(\ln \frac{1}{\bar{R}_{11}} + \ldots + \ln \frac{1}{\bar{R}_{1q}} - \ln \frac{1}{\bar{R}_{21}} - \ldots - \ln \frac{1}{\bar{R}_{2q}}\right) \end{aligned} \tag{7}$$

V_0: potential of uniform halfspace

I: current/length

C: position of current electrode

P: position of potential electrode

$\bar{R}_{rq}$: distance of current C and potential electrodes P_{rq}

r=1: positive electrode (subscript)

r=2: negative electrode (subscript)

q: number of electrode pairs (subscript)

$$V_c(\xi, \eta) = \sum_{m=1}^{\infty} \left(A_m^{(1)} \cos m\xi + B_m^{(1)} \sin \xi\right)\left(e^{m\eta} + e^{m\eta_0}\right) \tag{8}$$

V_c: potential of the cylinder

ξ, η: bipolar co-ordinates after LÖSCH et al. [1979]

A, B: integration constants

LÖSCH et al. [1979] proved by model measurements that if one applies line electrodes in a 2-D medium it results in quantitatively the same apparent resistivity values as point electrodes used in a 3-D medium. Appendix A presents some results of numeric investigations proving that the error caused by line electrodes in 2-D model calculations is smaller than 1%.

FERENCZY [1980] calculated the potentials of (7) and (8) for the case of dipole–dipole array with the assumptions that the electrodes are placed on the surface and the profile is perpendicular to the axis of the cylinder. Then the bipolar co-ordinates can be written as

$$\eta = 0 \tag{9}$$

$$\eta_0 = \ln\left(\frac{H}{R} + \sqrt{\frac{H^2}{R^2} - 1}\right) \tag{10}$$

$$\xi_q = 2\arctan\frac{\sqrt{H^2 - R^2}}{x_q} \tag{11}$$

x_q: co-ordinate of the q^{th} electrode along the profile
H, R: parameters of the 2-D model

Then the potentials in (7) and (8) for any arrays consisting of two current and two potential electrodes can be calculated as:

$$\Delta V_0 = \frac{I\rho_1}{2\pi}\left(\ln\frac{1-\cos\left(\xi_{P_1} - \xi_{C_2}\right)}{1-\cos\left(\xi_{P_1} - \xi_{C_1}\right)} - \ln\frac{1-\cos\left(\xi_{P_2} - \xi_{C_2}\right)}{1-\cos\left(\xi_{P_2} - \xi_{C_1}\right)}\right) \tag{12}$$

$$\Delta V_c = \sum_{m=1}^{\infty} \frac{2I\rho_1}{m\pi} \cdot \frac{\alpha}{e^{2m\eta_0} - \alpha} \cdot \left\{\left(\cos m\xi_{C_1} - \cos m\xi_{C_2}\right)\cdot\left(\cos m\xi_{P_1} - \cos m\xi_{P_2}\right) + \left(\sin m\xi_{C_1} - \sin m\xi_{C_2}\right)\cdot\left(\sin m\xi_{P_1} - \sin m\xi_{P_2}\right)\right\} \tag{13}$$

ρ_1: resistivity of the halfspace
ρ_2: resistivity of the cylinder

$$\alpha = \frac{\rho_2 - \rho_1}{\rho_2 + \rho_1}$$

The calculated resistivity curve of the 2-D model on *Fig. 1* can be determined from:

$$\frac{\rho_a}{\rho_1} = 1 + \frac{\Delta V_c}{\Delta V_0} \tag{14}$$

For models with more than one cavity the potential of the model can be calculated from the superposition of the anomalies of each cylinder (15), and the model resistivity can be written as (16):

$$\Delta V_s = \sum_{i=1}^{n_c} \Delta V_c^i + (n_c - 1)\Delta V_0 \tag{15}$$

$$\frac{\rho_a}{\rho_1} = 1 + \frac{\Delta V_s}{\Delta V_0} \tag{16}$$

ΔV_s: anomaly after superposition
ΔV_c^i: anomaly of i^{th} cylinder
n_c: number of cavities

Numeric investigations also prove that the effect of more cylinders can be correctly determined by the method of superposition (even in the case of cavities relatively close to each other) when the apparent resistivity is reached from separately calculated and stacked primary (ΔV_0) and secondary (ΔV_c) potentials (Appendix B).

Sensitivity investigations proved [NYÁRI 1997] that this method is not sensitive to the resistivity value of the cavity. At relative low resistivity contrast between the earth and the cavity (ρ_2=5ρ_1) fulfils the model assumption of infinite cylinder resistivity. For these purposes parameter ρ_2 was kept constant during the inversion process.

Qualifying of parameters

In order to qualify the calculated model parameters we followed the definitions of SALÁT et al. [1982]. When the data are uncorrelated the distribution of the model parameters can be characterized by the covariance matrix.

$$\underline{\underline{\mathrm{cov}}} = \sigma_d^2 \left(\underline{\underline{G}}^T \underline{\underline{G}} \right)^{-1} \tag{17}$$

$$\sigma_d = \sqrt{\frac{1}{m}\sum_{i=1}^{m}\left(\frac{Y^{obs} - Y^{calc}}{Y^{calc}}\right)^2}$$

m: number of data points

The diagonal elements of the covariance matrix give the uncertainty of the model parameters (variance). The off-diagonal elements describe the correlation of the parameters (18).

$$\mathrm{corr}_{ij} = \frac{\mathrm{cov}_{ij}}{\sqrt{\mathrm{cov}_{ii}\,\mathrm{cov}_{jj}}} \qquad (18)$$

corr_{ij}: correlation of i^{th} and j^{th} model parameters.

Numerical investigations

In order to test the inversion algorithm for geoelectric cavity detection synthetic data have been computed. The effect of different electrode arrays with four electrodes has also been investigated. OWEN [1983] found that dipole–dipole array is the most suitable configuration for the purpose of cavity detection. However at greater depths the separation of the dipoles is large in relation to the distance of the AB and MN electrodes so in such cases the measured data contain too high noise level. The effect of resistivity anomalies on different Wenner configurations has been observed by NYÁRI [1997] with the result that the conventional Wenner (AMNB) configuration can be used the most effectively for cavity detection. So the inversion method has been tested only with datasets of these two arrays.

Different levels of Gaussian noise have been added to the analytically calculated datasets representing low (2%) and high (5%) noise (*Figs. 2, 3*). *Table I* shows the parameters of the model used and the uncertainty of the estimation after the inversion. It can be observed that the uncertainties of resistivity and location parameters are the smallest in the case of both arrays. The errors of depth and size parameters were around the added noise level at dipole–dipole, and much higher than the noise level in the case of the Wenner array.

Field example

Near-surface cavities were detected in the village of Emőd in Hungary in 1987. The measurements were carried out by GYULAI et al. [1987]. A dipole–dipole array was applied with a = 2 m unit electrode spacing, and

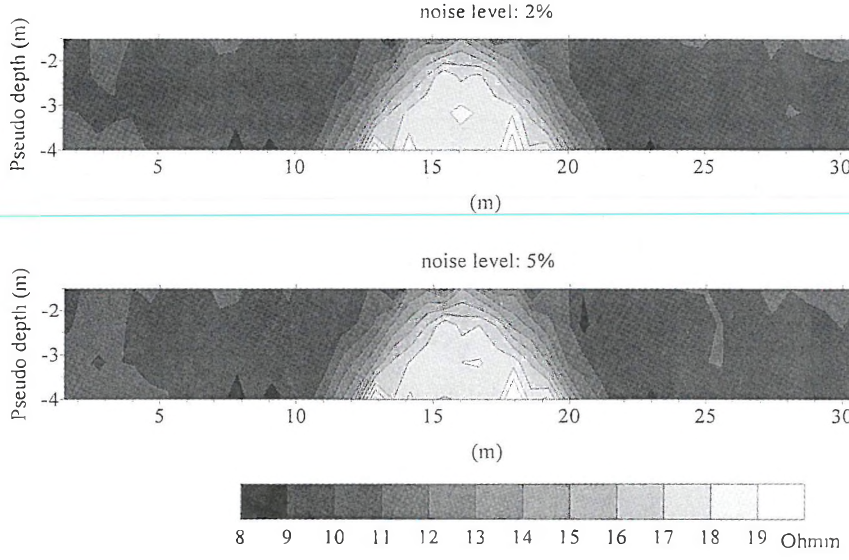

Fig. 2. Synthetic dipole–dipole pseudo sections with different noise level
2. ábra. Szintetikus dipól-dipól pszeudo szelvények különböző zajszintekkel

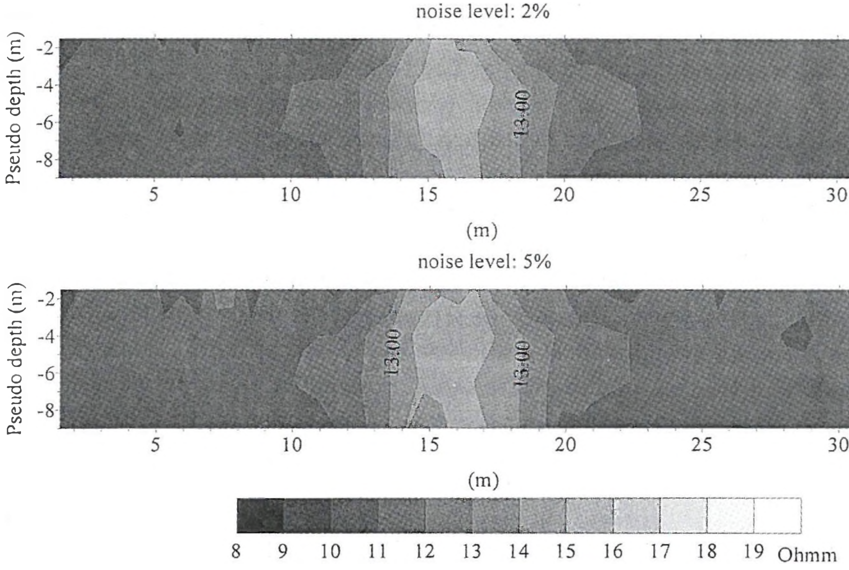

Fig. 3. Synthetic Wenner pseudo sections with different noise level
3. ábra. Szintetikus Wenner-pszeudo szelvények különböző zajszintekkel

Parameter	**Uncertainties of parameters (%)**			
	DD 2%	W 2%	DD 5%	W 5%
ρ_1=10 Ωm	0.34	0.59	0.48	0.8
H=3 m	3.05	7.54	4.39	10.84
R= 2 m	5.11	17.23	7.23	24.89
X=16 m	0.16	0.39	0.24	0.57

Table I. Model parameters and their uncertainties after single inversion of datasets with different noise and electrode array. *DD n%*: dipole–dipole data with *n*% of noise level; *W n%*: Wenner data with *n*% of noise level

I. táblázat. Modellparaméterek és bizonytalansági értékeik egyszeres inverzió után különböző zajszint és elektróda elrendezés esetén. *DD n%*: dipól-dipól adatok *n*% zajszint mellett; *W n%*: Wenner adatok *n*% zajszint mellett

n = 1,2,...,5 depth levels were investigated. *Figure 4* shows the measured data. The result of the inversion is presented in *Table II*. It is interesting that the uncertainties of parameters *H* and *R* are smaller than the fitting error (13.8 %) of the measured and the calculated datasets.

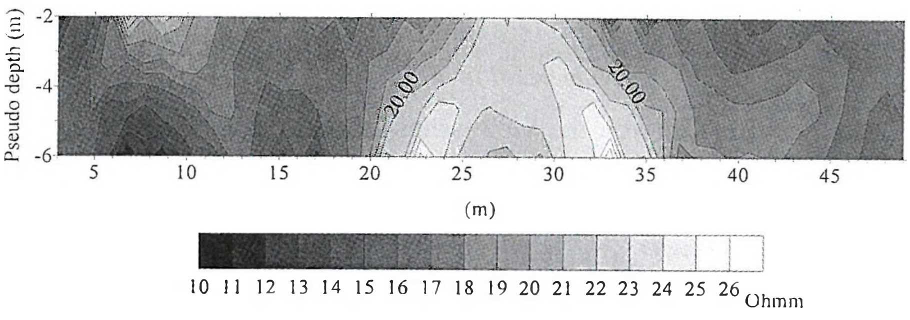

Fig. 4. Resistivity profile measured at Emőd
4. ábra. Emődnél mért ellenállászelvény

Parameters	$\tilde{n}_1$	*H*	*R*	*X*
Inverted values	16.8 Ωm	3.6 m	2.2 m	28.1 m
Uncertainties	1%	8%	8%	0%

Table II. Inversion result of resistivity profile measured at Emőd. Fitting error: 13.8%
II. táblázat. Az Emőd mellett mért ellenállásszelvény inverziós eredménye

3. Data processing with simultaneous inversion

The algorithm of simultaneous inversion is quite similar to simple inversion. The main difference is that the $\bar{s}$ vector of the measured data has two different parts depending on the arrays applied in the measurement:

$$\bar{s} = \bar{s}_1 + \bar{s}_2 \tag{19}$$

$\bar{s}_1$: vector of data measured with the first array

$\bar{s}_2$: vector of data measured with the second array.

GYULAI [1998] investigated the parameter sensitivities of some arrays. He observed that the sensitivity of geometric parameters (length, width, depth) does not change equally with different arrays. This means that one array is more sensitive for width, the other for length, etc. So if one applies two different arrays in one inversion process the whole dataset will be sensitive to both parameters.

The dipole–dipole array has almost the best horizontal resolution among the electrode configurations. However it can be applied only for detecting a small depth range because of the high noise level caused by the separation rate of the electrodes. With a Wenner array one can investigate a larger depth scale but with worse horizontal resolution. It is assumed that if one uses these two arrays together in inversion processing the uncertainties of the inverted parameters can be decreased.

Numerical investigations

The synthetic data were the same as those used in testing the simple inversion method. *Table III.* shows the errors of the model parameters of *Table 1* af-

Parameter	**Uncertainties of parameters (%)**		
	DD 2%, W 2%	**DD 5%, W 5%**	**DD 5%, W 2%**
ρ_1=10 Ωm	0.28	0.40	0.35
H=3 m	2.39	3.42	2.97
R= 2 m	4.36	6.2	5.38
X=16 m	0.15	0.22	0.19

Table III. Model parameters and their uncertainties after simultaneous inversion of datasets with different noise and electrode array. *DDn%*: dipole–dipole data with *n*% of noise level; *Wn%*: Wenner data with *n*% of noise level

III. táblázat. Modellpraraméterek és bizonytalansági értékeik az adatok szimultán inverziója után különböző zajszintek és elektróda elrendezések esetén. *DDn%*: dipól–dipól adatok *n*% zajszint mellett; *Wn%* Wenner adatok *n*% zajszint mellett ter simultaneous inversion. It can be observed that the errors of all parameters were smaller at both noise levels than in the errors in *Table 1*.

In the next step datasets based on real field data acquisition have been computed. This means that the dipole–dipole data contained higher noise (5%), than the Wenner data (2%). The errors of the parameters after simultaneous inversion are also presented in Table III. It is remarkable that even the noisy dipole–dipole data could reduce the uncertainties of the Wenner data as well. *Figures 5* and *6* respectively present how simultaneous inversion can reduce the errors of parameters *H* and *R*.

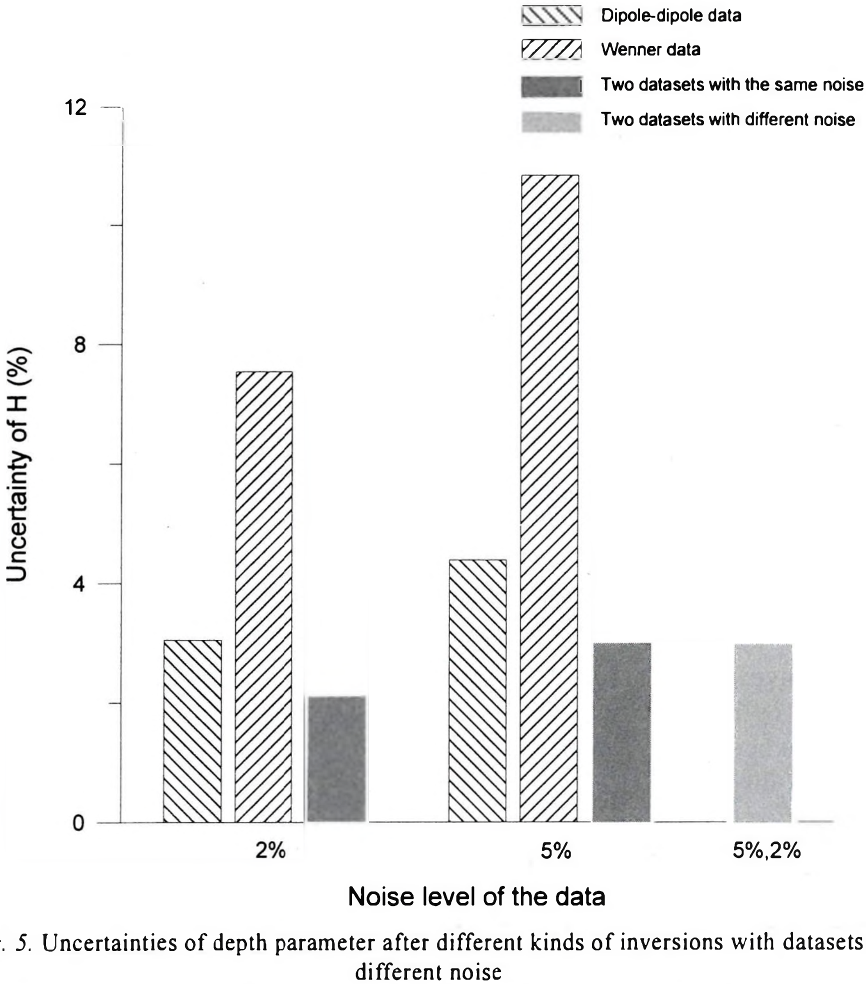

Fig. 5. Uncertainties of depth parameter after different kinds of inversions with datasets of different noise

5. ábra. A mélységparaméterek bizonytalanságai különböző inverziók után eltérő zajok mellett

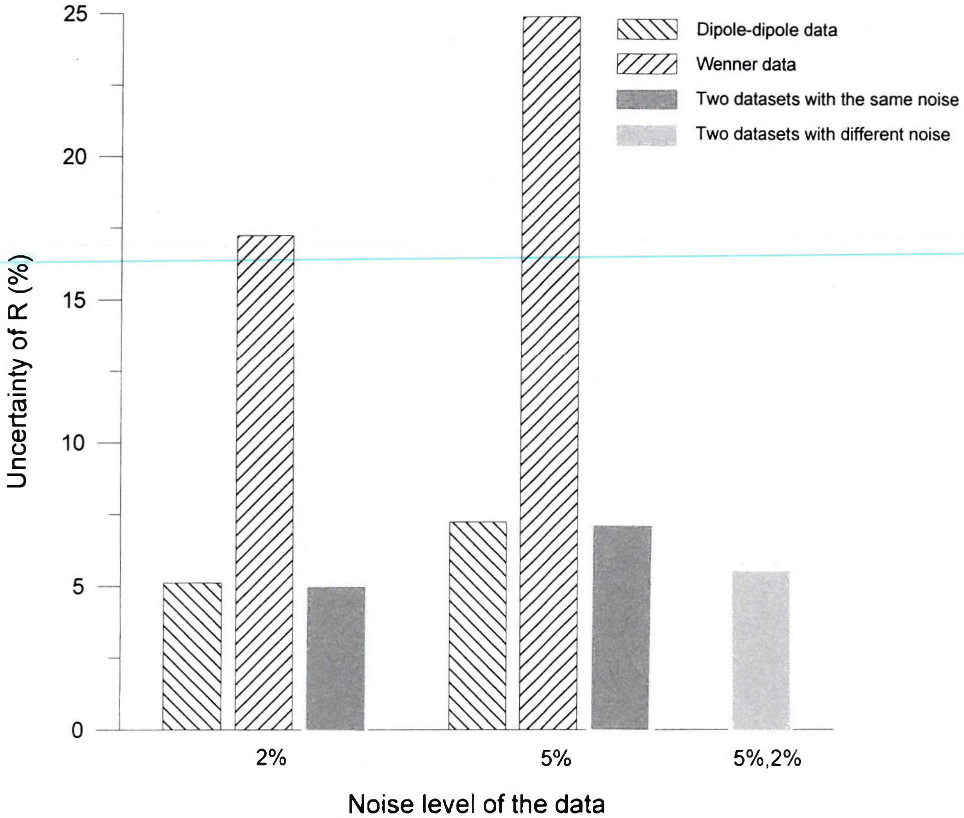

Fig. 6. Uncertainties of radius parameter after different kinds of inversions with datasets of different noise

6. ábra. A sugárparaméterek bizonytalansági értékei eltérő zajokkal terhelt adatrendszerek különböző inverziói után

To investigate the inversion method in the case of more cavities a model with two cylinders with the same H/R ratio (H/R=1.3) but different size and depth has been used. *Table IV* presents the model and qualifying parameters when the distance between the objects is relatively large. The results of the single inversion show that the reliability of the parameter estimation is better for the cylinder with shallower depth in the case of dipole–dipole, and for the cylinder with greater depth in the case of the Wenner array. If the two cylinders

V. táblázat. Modellparaméterek és bizonytalansági értékeik egyszeres és szimultán inverzió után különböző zajszintekre és eletktróda elrendezésekre egymáshoz közel lévő két henger esetén. *DD n%*: dipól-dipól adatok *n*% zajszint mellett; *W n%*: Wenner adatok *n*% zajszint mellett

Qualifying parameter	Model parameter	M1 model	DD 2%	W 2%	DD 5%	W 5%	DD 5%, W 2%
Uncertainty [%]	ρ_1	10 Ohmm	0.396	0.79	0.577	1.122	0.433
	H_1	4 m	5.198	12.97	7.625	19.58	4.747
	R_1	3 m	7.06	21.6	10.275	33.486	6.872
	X_1	10 m	0.421	1.11	0.62	1.708	0.507
	H_2	2 m	3.635	14.15	5.337	21.428	4.379
	R_2	1.5 m	6.279	27.95	9.319	44.455	7.724
	X_2	20 m	0.13	0.37	0.191	0.556	0.157
Fitting error [%]			4.21	4.33	6.131	6.173	5.393
Rel. model distance [%]			1.978	1.731	0.955	1.213	0.485
Number of data			177	147	177	147	324

Table IV. Model parameters and their uncertainties after single and simultaneous inversion of datasets with different noise and electrode array for two cylinders that are relatively far apart. *DD n%*: dipole–dipole data with *n*% of noise level; *W n%*: Wenner data with *n*% of noise level.

IV. táblázat. Modellparaméterek és bizonytalansági értékeik egyszeres és szimultán inverzió után különböző zajszintekre és eletktróda elrendezésekre egymástól viszonylag távol lévő két henger esetén. *DD n%*: dipól-dipól adatok *n*% zajszint mellett; *W n%*: Wenner adatok *n*% zajszint mellett

Qualifying parameter	Model parameter	M2 model	DD 2%	W 2%	DD 5%	W 5%	DD 5%, W 2%
Uncertainty [%]	ρ_1	10 Ohmm	0.381	0.668	0.551	0.944	0.395
	H_1	4 m	5.675	14.437	8.314	20.88	5.028
	R_1	3 m	7.616	23.452	10.882	64.03	7.194
	X_1	12.5 m	0.404	1.208	0.598	1.816	0.483
	H_2	2 m	4.24	18.999	6.346	30.831	5.314
	R_2	1.5 m	7.156	35.743	10.816	61.233	9.905
	X_2	18 m	0.163	0.526	0.244	0.761	0.202
Fitting error [%]			4.212	4.289	6.054	6.093	5.345
Rel. model distance [%]			0.588	1.768	2.548	6.882	1.391
Number of data			177	147	177	147	324

Table V. Model parameters and their uncertainties after single and simultaneous inversion of datasets with different noise and electrode array in the case of two close cylinders. *DD n%*: dipole–dipole data with *n*% of noise level; *W n%*: Wenner data with *n*% of noise level.

are sited close to each other the reliability values of the model parameters become worse (*Table V.*). On applying the simultaneous inversion method the closest estimation of the parameters can be reached in both cases.

4. Conclusions

If one processes resistivity data by means of analytical inversion the location, depth and size of the cavities along the profile can be reliably defined. The best estimation of these parameters can be achieved from data measured with a dipole–dipole array. To reduce the errors of the investigated parameters it is advisable to measure both dipole–dipole and Wenner arrays for simultaneous inversion.

Acknowledgement

This paper presents the results of an OTKA research project Nr T25370.

Appendix A

During the analytic calculations the apparent resistivity values of 2-D models are determined by applying the formulae of line sources though in practice the measurements are carried out with point sources. To investigate the model error caused by that kind of calculation the results of analytic model calculations were compared with the results of 2.5-D FD calculations using the same model and measuring parameters. The only difference between the models of the two kinds of calculation was their shape: a cylinder was used for analytic and a rectangle for FD modelling. The theory of 2.5-D calculations has been improved by PRÁCSER [1998]. The difference of the two datasets always stayed below 1% containing not only the difference of the sources but the difference in the shape of the objects as well. *Figure 7* shows an example model for such comparison. The difference between the two complete datasets (with $n = 1, \ldots, 8$) was 0.987%.

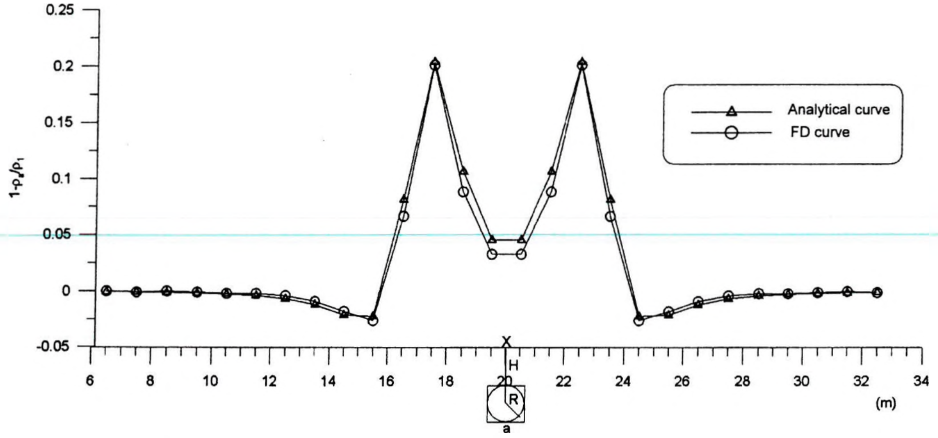

Fig. 7. Example model for investigating the error caused by using line sources instead of point sources. Electrode array: dipole–dipole, unit electrode distance: 1 m, n=5. Model parameters: ρ_2/ρ_1=100, H=1.5 m, R=0.5 m, a=1 m, X=20 m

7. ábra. Példa a pont- és vonalforrások használata miatti eltérés vizsgálatához alkalmazott modellre. Elektróda elrendezés: dipól–dipól, egységnyi elektróda távolság: 1 m, n=5. Modellparaméterek : ρ_2/ρ_1=100, H=1,5 m, R=0,5 m, a=1 m, X=20 m

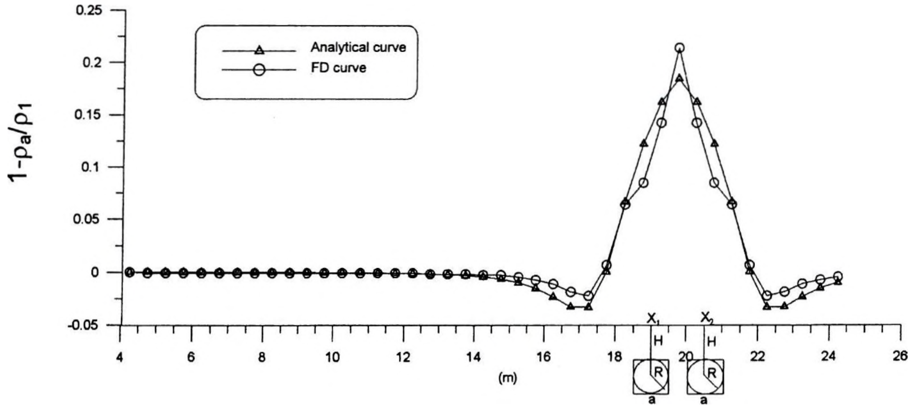

Fig. 8. Example model and theoretical curves for investigating the application of the theory of superposition in the case of two cavities. Electrode array: dipole–dipole, unit electrode distance: 0.5 m, n=5. Model parameters: ρ_2/ρ_1=100, H=1.5 m, R=0.5 m, a=1 m, X_1=19 m, X_2=20.5 m

8. ábra. Példa a szuperpozíció elve alkalmazhatóságának vizsgálatához használt két üreges modellre és elméleti görbékre. Elektróda elrendezés: dipól–dipól, egységnyi elektróda távolság: 0,5 m, n=5. Modellparaméterek: ρ_2/ρ_1=100, H=1,5 m, R=0,5 m, a=1 m, X_1=19 m, X_2=20,5 m

Appendix B

The geoelectric effect of two or more horizontal cylinders is calculated analytically by using the theory of superposition. Numeric investigations proved that this theory can be correctly used when the apparent resistivity is determined from separately calculated primary (caused by uniform halfspace) and secondary (caused by the cylinder) potentials. The control models were calculated after PRÁCSER [1998], as in App. A. In the case of cavities separated by only one distance unit from each other (*Fig. 8*) the difference of the two datasets (with $n = 1,\dots,10$) was 2.54%. If one increased the distance between the objects the difference between the analytical and FD values strongly decreased.

REFERENCES

BARKER R. D. 1992: A simple algorithm for electrical imaging of the subsurface. First Break **10**, pp. 53–62

DEY A., MORRISON H. F. 1979: Resistivity modeling for arbitrarily shaped two-dimensional structures. Geophysical Prospecting **27**, pp. 106–136

DOBRÓKA M., GYULAI Á., ORMOS T., CSÓKÁS J., DRESEN L. 1991: Joint inversion of seismic and geoelectric data recorded in an underground coal mine. Geophysical Prospecting **39**, pp. 644–665

FERENCZY L. 1980: Determination of depth and dimension of near-surface cavities by means of geoelectric dipole profiling (in Hungarian). Magyar Geofizika **XXI**, 4, pp. 134–142

GYULAI Á., FERENCZY L., TAKÁCS E. 1987: Report of geophysical cavity detection having been carried out in village Emőd in connection with planning waste water canal. (in Hungarian). Report, Miskolci Egyetem Geofizikai Tanszék

GYULAI Á. 1996–97: Cavity and void detection using 1.5-D inversion methods (in Hungarian). III. report (OTKA T019088) Miskolci Egyetem Geofizikai Tanszék

GYULAI Á. 1998: Some aspects of cave research using geoelectric method (in Hungarian). Magyar Geofizika **39**, 2, pp. 43–50

LOKE M. H., BARKER R. D. 1996: Rapid least squares inversion of apparent resistivity pseudosections by a quasi-Newton method. Geophysical Prospecting **44**, pp. 131–152

LÖSCH W., MILITZER H., RÖSLER R. 1979: Zur geophysikalischen Hohlraoumortung mittels geoelektrischer Widerstandmethoden. Freiberger Forschungshefte C341, pp. 53–126

NYÁRI Zs. 1997: Examination of the possibilities of geoelectric cavity exploration using analytical modelling (in Hungarian). Magyar Geofizika **38**, 3, pp. 194–204

OWEN T. E. 1983: Detection and mapping of tunnels and caves. Development in geophysical exploration methods-5, Applied science Publishers London

SALÁT P., CSEREPES L., TARCSAI Gy., VERMES M., DRAHOS D. 1982: Statistical characteristics of information of geophysical interpretation (in Hungarian). Tankönyvkiadó Budapest

Üregkutatási célú fajlagos ellenállás mérések minőség ellenőrzött inverziója

Nyári Zsuzsanna

Üregkutatási feladatok mindennaposak a mérnökgeofizikai gyakorlatban. A fajlagos ellenállás mérésén alapuló módszereket a sokelektródás mérési rendszerek kifejlesztése óta széles körben alkalmazzák ilyen feladatok megoldására. Az új, számítógép vezérlésű adatgyűjtő rendszerek lehetővé teszik nagy mennyiségű adat rövid időn belül történő regisztrálását. A dolgozat olyan elméleti fejlesztések eredményeit ismerteti, melyek a későbbiek során alkalmazhatóvá válnak az ELGI keretében végzett felszínközeli üregkutatási feladatok megoldásában.

Az üregek lokalizálásán túl gyakran szükséges azok méretét és mélységét is megadni Kifejlesztettünk egy 2-D-s analitikus modellezésen alapuló inverziós módszert, amely az üreg helyének, mélységének és méretének számszerű értékét eredményezi, és mindezek mellett meghatározza a számított paraméterek valószínű hibáját is. A módszert sikeres numerikus tesztelése után terepi példán is alkalmaztuk.

Szimultán inverziós módszert fejlesztettünk ki annak érdekében, hogy csökkentsük az eredményül kapott modellparaméterek hibáját. Az eljárás két, különböző elektróda elrendezéssel (dipól–dipól, Wenner) mért adatrendszer együttes inverzióját végzi el. A numerikus vizsgálatok alapján kijelenthető, hogy ez az eljárás valóban megbízhatóbb paramétereket eredményez, mint a hagyományos inverzió.

ABOUT THE AUTHOR

Zsuzsanna Nyári graduated as a geophysical engineer from the University of Miskolc in 1994. She continued her post-graduation studies at the University in 1995. Then she joined the Division of Engineer Geophysics of ELGI. Topics of her main activity: electric and geoelectric field measurements and data processing in the field of engineering geophysics, development of geoelectric data processing.